A High Efficiency High Power-Density LLC DC-DC Converter for Electric Vehicles (EVs) On-Board Low Voltage DC-DC Converter (LDC) Application

Xiang Zhou, *Member*, *IEEE*; Bo Sheng, Student *Member*, *IEEE*; Wenbo Liu, Student *Member*, *IEEE*; Yang Chen, *Member*, *IEEE*; Andrew, Yurek, *Student Member, IEEE*; Yan-Fei Liu, *Fellow*, *IEEE*; P. C. Sen, *Life Fellow*, *IEEE*;

Department of Electrical and Computer Engineering
Queen's University
Kingston, Canada
xiang.zhou@queensu.ca, bo.sheng@queensu.ca, liu.wenbo@queensu.ca, yang.chen@queensu.ca, 13aty@queensu.ca, yanfei.liu@queensu.ca, senp@queensu.ca

K. Lakshmi Varaha Iyer

Magna International Inc.,
Aurora, ON, Canada

LakshmiVaraha.Iyer@magna.com

***Abstract*-This paper presents a high efficiency high power-density LLC DC-DC converter for Electric Vehicles (EVs) on-board low voltage DC-DC converter (LDC) application. In the proposed LDC, primary switches achieve ZVS turn-on and secondary synchronous rectifier switches achieve ZVS turn-on and ZCS turn-off. To reduce current stress and improve efficiency, three phase interleaved LLC DC-DC converters are paralleled to provide more than 200A load current. Switch-Controlled Capacitor (SCC) technology is used to achieve the load current sharing of the three phase LLC DC-DC converter. In addition, GaN HEMTs are used in the transformer primary to improve the switching frequency and power-density. To verify the analysis, a 3.8kW(14V/270A) LLC DC-DC converter prototype is designed. The experimental results show that full load efficiency is 95.8% at 270A load current and 3kW/L power-density is achieved.**

I. Introduction

Recently, Electric Vehicles (EVs) are attracting increased attention as they are more environmentally friendly and cheaper than fossil fuels vehicles [1]. As shown in Fig. 1, the battery system of EVs always consist of high voltage (HV) Li-Ion batteries (200V~450V) and low voltage (LV) Lead-acid batteries (9V~16V). In general, HV batteries are used for traction motor drives. LV batteries are used in the auxiliary power supply for lighting, audio/video systems, air conditioners, automatic seats, etc,. The HV battery is usually charged from the grid by the off-board charger or the on-board charger. The LV battery is usually charged from the HV battery by using a low-voltage DC-DC converter (LDC). In general, galvanically isolated DC-DC converters are required in LDC to ensure safety and achieve high step down voltage ratio (430V~9V).

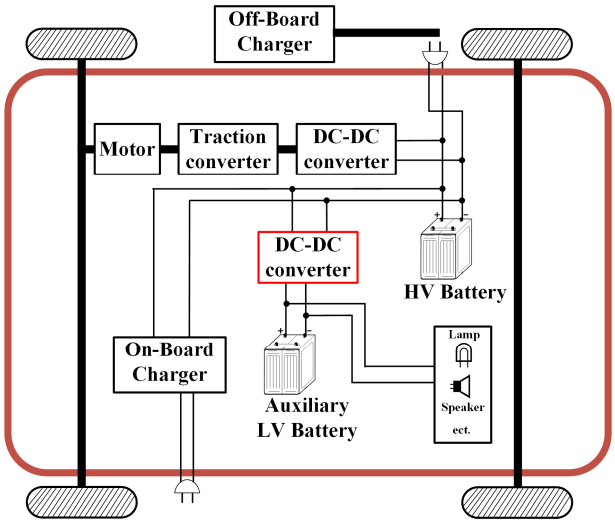

Fig. 1. Diagram of EV power train

In [1], phase-shift full bridge converter is adopted in LDC, which is also used as the active filter (AF) circuit to mitigate the second-order harmonic current existing on the dc-link after the power factor correction (PFC) converter when HVB is charged and LVB is not charged. To guarantee ZVS of the primary switches in the phase-shift full bridge converter LDC, auxiliary inductors are used in

978-1-7281-4829-8/20/$31.00 ©2020 IEEE

[2]-[4]. In [5], a built-in buck circuit is use in the LDC secondary to solve the induced voltage caused by the multi-winding high-frequency transformer.

In [1]-[5], the phase-shift full bridge DC-DC converter is used for LDC. As load current is very high, a current-doubler circuit is usually utilized in the transformer secondary to reduce current stress and improve efficiency [1]-[3]. However, compared to a phase-shift full bridge DC-DC converter, ZVS of primary switches and ZCS of secondary switches can be achieved easily in the LLC resonant converter [6]-[8].

Along with increased electrical equipment required in EVs, auxiliary power supplies with small package volume and greater than 2.5kW power rating are necessary. This means more than 200A output current should be provided in LDC with a higher power-density. Therefore, synchronous rectification (SR) is usually adopted to reduce transformer secondary conduction loss in LLC DC-DC converter. Recently, wide bandgap devices (such as SiC or GaN) are used in switching power supplies to improve efficiency and power-density of the circuit.

In this paper, a three-phase interleaved LLC DC-DC converter operating in parallelis designed for LDC to reduce transformer secondary current stress. Switch-Controlled Capacitor (SCC) technology is used to achieve current sharing among the three LLC DC-DC converter phases [10]. In addition, GaN HEMTs are used in the primary side to reduce switching loss and conduction loss at high switching freqeuncy and to increase power-density of the LDC. Thus, high efficiency (95.8% at 270A full load, 96.5% peak efficiency at 160A load current) and high power-density (3kW/L) are achieved at same time in the presented LDC for EVs.

This paper is organized as following. Section II illustrates current sharing strategy. Section III gives parameters design. In addition, simulation analysis is presented in Section IV. Transformer design is given in Section V. Section VI and VII give experimental results and conclusion.

II. Current Sharing Strategy

Due to the tolerance of the resonant inductor and resonant capacitor values among three phase LLC converters, the current stress is the highest in the lowest impedance phase. When load current is large, the loss of the lowest impedance phase will be high. To solve this problem, SCC technology is used to achieve current sharing in the proposed LDC circuit.

For example, in the first phase, capacitor C_{a1} is paralleled with switches S_1 and S_2 as shown in Fig. 2. If switches S_1 and S_2 are turned on all the time, the resonant tank consists of resonant capacitor C_{r1} and resonant inductor L_{r1}. If switches S_1 and S_2 are turned off all the time, capacitor C_{a1} is in series with capacitor C_{r1}, and the equivalent resonant capacitor $C_{r,eq}$ is smaller than C_{r1}. Therefore, the equivalent resonant capacitor can be controlled, as shown in (2). Thus, the error of three phase resonant parameter can be adjusted, and load current of three phase circuit is balanced by adjusting the conduction angle of SCC switches in the proposed LDC.

As shown in Fig. 3, when current i_{SCC} is positive, switch S_2 is turned on, and when current i_{SCC} is negative, switch S_1 is turned on. It can be known from Fig. 3 that switches S_1 and S_2 can always achieve ZVS turn-on. The conduction phase angle α depends on the turn-on time and turn-off time of switches S_1~S_2. Similarly, S_3~S_6 also can achieve ZVS turn-on.

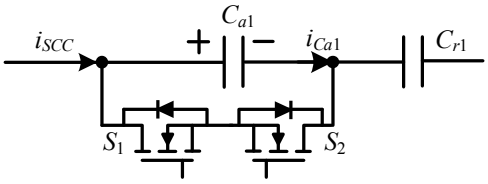

Fig. 2. Switch-controlled capacitor (SCC) circuit

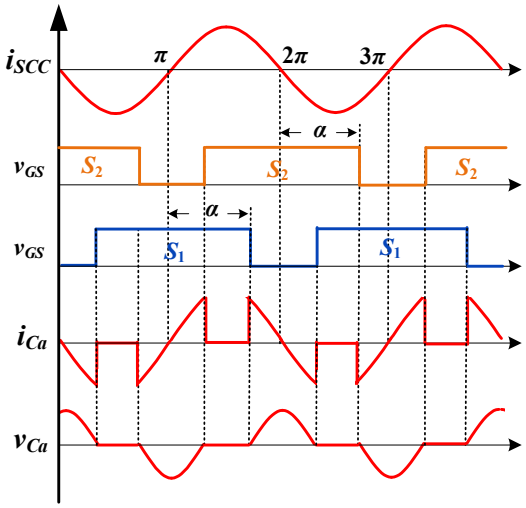

Fig. 3. SCC control strategy

The equivalent value of the switch-controlled-capacitor can be calculated as

$$C_{SC}=\frac{C_a}{2-(2\alpha-\sin 2\alpha)/\pi}. \quad (1)$$

And the equivalent resonant capacitor $C_{r,eq}$ is

$$C_{r,eq}=\frac{C_{SC}C_r}{C_{SC}+C_r}=\frac{C_aC_r}{C_a+C_r[2-(2\alpha-\sin 2\alpha)/\pi]}. \quad (2)$$

The voltage gain of the LLC DC-DC converter is

$$M=\frac{nV_o}{V_{in}}=\frac{K}{\sqrt{\left[(\frac{\omega_r}{\omega_s})^2-K-1\right]^2+\frac{(\pi^2\omega_sL_p)^2}{64N^4R_L^2}\left[(\frac{\omega_r}{\omega_s})^2-1\right]^2}}. \quad (3)$$

where $K=\frac{L_p}{L_r}$,

$\omega_s=2\pi f_s$, $\omega_r=\frac{1}{\sqrt{L_rC_{r,eq}}}$ and N is turns ratio of transformer.

When three phase LLC converters are adopted with input-parallel output-parallel, the input voltage and output voltage are the same in three phase converters. From (3), load current can be sharing under same input output voltage gain by adjusting equivalent resonant capacitor $C_{r,eq}$ in three phase converters. Thus, if we design three phase LLC DC-DC converter with input-parallel output-parallel and 270A load current by using SCC technology, the resonant parameters design is similar with sing phase LLC DC-DC converter with 90A load current.

Based on the above analysis, a three-phase interleaved LLC converter is designed in this paper. In the proposed converter with SCC technology, there are two advantages: 1) load current sharing is achieved among multi-phase converters. 2) wide input and output voltage range is realized with 0.5 duty cycle of primary switches, and ZVS of primary switches and SCC switches are achieved. 3) the switching frequency of the converter with 90A load current is higher than that of the converter with 270A load current, which benefits from small magnetics components and high power-density.

III. Parameters Design

In this LDC design, the load current is 270A. Consequently, the conduction loss of the transformer secondary is very high by using a single-phase converter; thus the efficiency of the circuit is decreased. The SR conduction loss of single-phase circuit is

$$P_{SR\_loss\_single}=(\frac{270\times\pi}{2\sqrt{2}})^2R_{ds(on)}. \quad (4)$$

If three LLC converters are connected in parallel to provide 270A load current by using SCC circuit, each LLC converter will provide 90A.

When two transformers are adopted in each LLC converter phase with input-series output-parallel, because the primary current of two transformers are the same and magnetizing current of two transformers are approximate, the secondary current of two transformers are the same. Therefore, 45A load current flows through each transformer. For a given SR R_{dson} at the same load current condition, total SR conduction loss of the three phases is

$$P_{SR\_loss\_three}=(\frac{45\times\pi}{2\sqrt{2}})^2R_{ds(on)}\times 6. \quad (5)$$

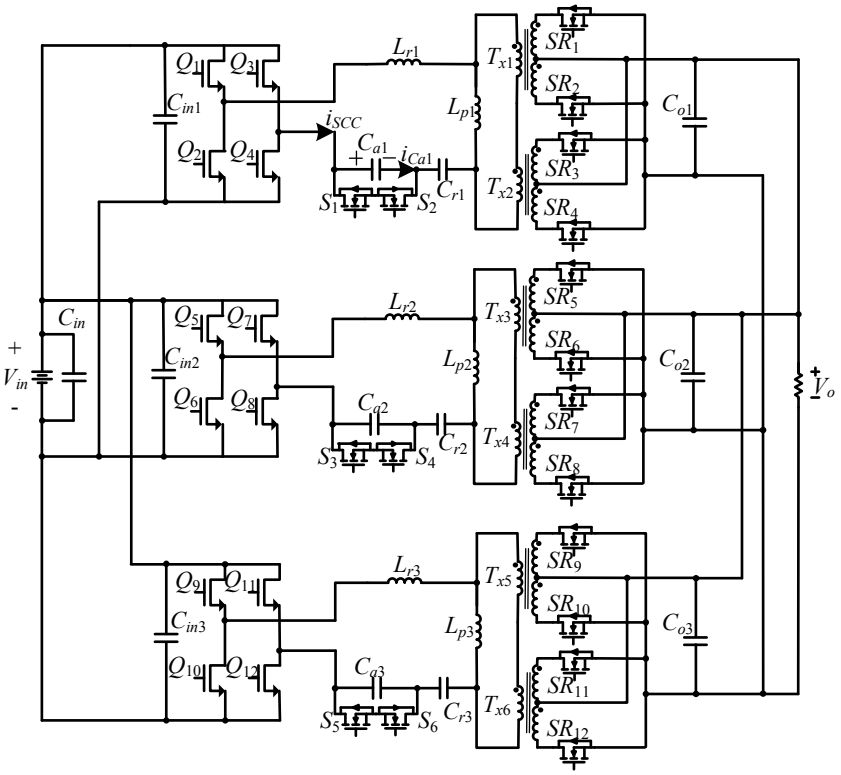

Fig. 4. The proposed LDC circuit

From (4) and (5), the conduction loss of a single-phase circuit is 6 times greater than a three-phase circuit. To reduce the copper loss of magnetic components as well as conduction loss of the transformer secondary, the proposed LDC for EVs adopts three phase interleaved LLC DC-DC converters to improve efficiency of the circuit, as shown in Fig. 4. Moreover, two transformers with primary side connected in series and secondary side connected in parallel are used in each phase LLC DC-DC converter to reduce current stress of SRs. Switches Q_1~Q_{12} use GaN HEMTS, therefore high switching frequency and high power-density are achieved in the proposed LDC.

Each phase of the LLC DC-DC converter considers 90A load operation for resonant parameter design.

To ensure the converter operates in the ZCS region of the SR, the resonant point (unity voltage gain) is selected based on the maximum input voltage and the minimum output voltage. The transformer turns ratio is determined by,

$$n = N_p : N_s = V_{in\_max} : V_{o\_min} \tag{6}$$

Where, N_p is the primary turns and N_s is the secondary turns number.

With 430V maximum input and 9V minimum output voltage, each transformer turns ratio should be 430V / 9V / 2 = 23.8. However, as 9V is an odd point with less current requirement, the turns ratio is selected as 22:1:1 for each transformer.

In the proposed LDC, wide input voltage (250V~430V) and output voltage (9V~16V) range are required. Because 250V input and 16V output is maximum step-up voltage gain point, the resonant parameters are designed for this condition. In the studied case, load capacity is different at different input condition. For 320V to 430V, the converter is rated for full power, while for 250V to 320V input voltage, only 60% load current is required.

As only 60% load current is needed at 250V input voltage, voltage gain should satisfy

$$M = \frac{K}{\sqrt{\left[(\frac{\omega_r}{\omega_s})^2 - K - 1\right]^2 + \frac{(\pi^2 \omega_s L_p)^2}{64 n^4 R_L^2}\left[(\frac{\omega_r}{\omega_s})^2 - 1\right]^2}} > \frac{16\times 44}{250} = 2.82. \tag{7}$$

Compared with 100kHz~200kHz resonant frequency in general LDC, the resonant frequency between L_r and C_r is selected close to 500kHz to reduce the volume of magnetic components and improve the power-density in this work. The selection of L_p is a tradeoff between the voltage gain (current capacity) and efficiency. A major barrier for high current LLC converter design is that L_p inductance should be controlled to be small to fulfill high voltage gain requirement. High circulation current will be induced when the L_p value is small and this high current can increase the conduction loss on primary side. However, since the primary current is very low as compared to the secondary, and GaN switches are used with superior low R_{dson} and switch loss. Therefore, the overall efficiency is not significantly sacrificed with a small L_p to cover the full range of gain requirement.

In order to satisfy (7), L_r=25uH, C_r=3.4nF and L_p= 125uH are selected in the proposed LDC. In this case, the diagram of the voltage gain is shown as Fig. 5.

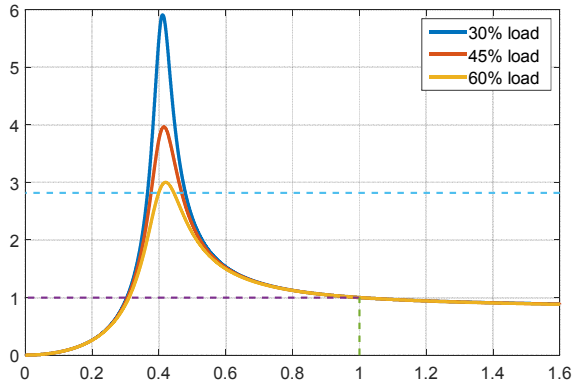

Fig. 5. Voltage gain of the proposed LDC

As shown in Fig. 5, 2.82 times step-up voltage gain is realized under 60% load current, which verifies the correction of the proposed resonant parameters.

IV. Simulation Analysis

According to the designed parameters, a simulated circuit is established by using PSIM simulation software. The simulation results are shown in Figs. 6–8.

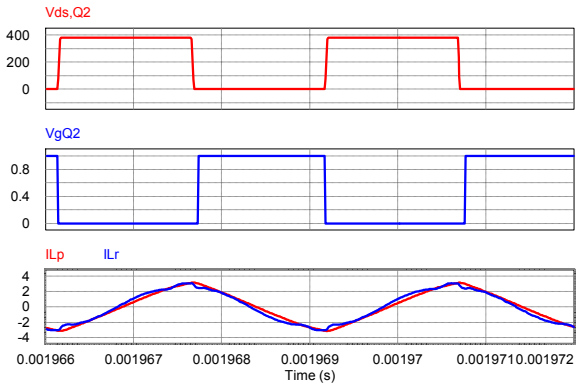

(a) when V_{in} is 380V, V_{out} is 14V and load current is 10A

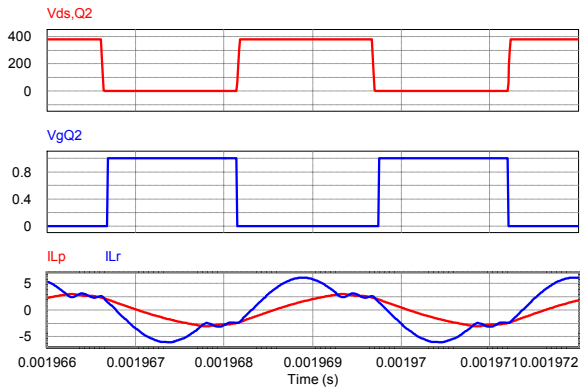

(b) when V_{in} is 380V, V_{out} is 14V and load current is 90A

Fig. 6. ZVS of primary switches at light load and full load

As shown in Fig. 6(a) and (b), ZVS turn-on of primary switches can be achieved at light load until full load wide load range, which reduces switching loss of primary switches and improves efficiency.

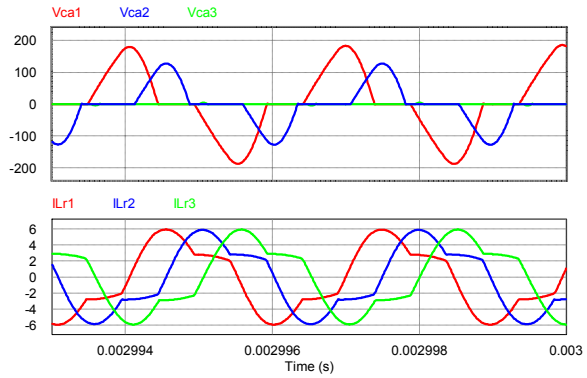

Fig. 7. Waveform of capacitor voltage v_{Ca1}, v_{Ca2}, v_{Ca3} and resonant inductor current i_{Lr1}, i_{Lr2}, i_{Lr3}

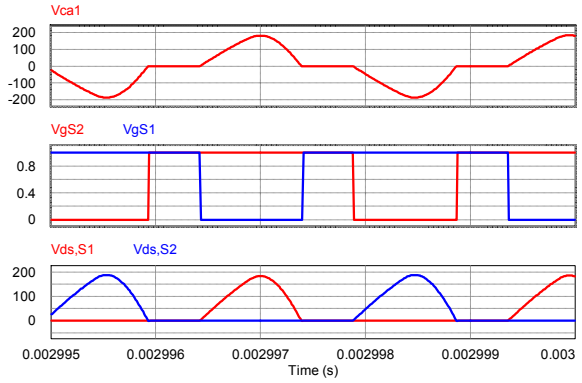

Fig. 8. Waveform of SCC circuit

In the simulated LDC circuit, parameter tolerances are predefined in each of the three-phases to verify the current sharing in the worst case. The first phase parameters are $1.05L_r$, $1.03L_p$, $1.05C_r$; the second phase parameters are L_r, L_p, C_r; and the third phase parameters are $0.95L_r$, $0.97L_p$, $0.95C_r$. As shown in Fig. 7, when V_{in} is 380V, V_{out} is 14V and 270A load current, by adjusting different α degree in SCC circuit, three phase resonant currents i_{Lr1}, i_{Lr2} and i_{Lr3} are 3.86A, 3.84A, and 3.82A respectively, which are very balanced among three phase circuits.

As shown in Fig. 8, switches S_1 and S_2 in SCC circuit achieve ZVS turn-on and turn-off, thus there is only conduction loss in SCC circuit, which has a very small effect on the efficiency of the LDC compared with the converter without SCC circuit.

V. Transformer Design

Since a considerable loss factor of the magnetic components is the high current stress on the transformer secondary winding, transformer design is an important consideration.

With the high operating frequency, the skin depth δ is very small, which will introduce high AC resistance into the winding with thick foil. The skin depth δ is 0.12mm at 300kHz frequency, so a three-layer laminated 0.25mm copper foil is used instead of a 0.75mm single layer thick copper foil as the secondary winding.

To reduce core loss of transformer, small maximum delta flex density ΔB_{max} is required. PQ3535 core and 3C97 material is adopted in the transformer. Litz wire is used to implement the magnetics to reduce the AC losses caused by skin effect and proximity effect. The primary winding is achieved using 22 turns of 2 layers of litz wire with 650 strands, and 1.8mm outside diameter (NELC650/44SN). The secondary windings are created using a three-layer 20mm × 0.25mm copper foil.

The maximum flex density of the transformer B_{max} is

$$B_{\max}=\frac{NV_o\frac{T_s}{4}}{NS}=\frac{V_oT}{4S}=\frac{14\times3.3\times10^{-6}}{4\times190\times10^{-6}}=61mT. \quad (8)$$

The L_r is realized using 15 turns of 3 layers of litz wire with 650 strands, and1.8mm outside diameter (NELC650/44SN). The L_p is realized using 44 turns of 4 layers of litz wire with 1100 strands, and 1.5mm outside diameter (NELC1100/48SN). The core size and material of all the magnetics are shown in Table. I.

TABLE I: CORE SIZE AND MATERIAL OF MAGNETICS

Inductor L_r		Inductor L_p		Transformer	
Core Size	Material	Core Size	Material	Core Size	Material
PQ32/20	3C97	PQ35/35	3C97	PQ35/35	3C97

Fig. 9 shows the diagram of the primary side and secondary side of the transformer.

(a) primary side

(b) secondary side

Fig. 9. Diagram of the transformer

VI. Experimental Results

To verify the analysis, a 14V/270A (3.8kW) prototype is designed and tested. The series resonant inductor L_r is 25μH, the parallel resonant inductor L_p is 125μH, the resonant capacitor C_r is 3.3nF, the SCC capacitor is 15nF and the transformer turns ratio is n_p:n_{s1}:n_{s2}=22:1:1. Fig. 10 shows the prototype of the proposed LDC, length, width and height of the prototype are 18.5cm, 13.5cm and 4.8cm, respectively, and 3kW/L power density is achieved.

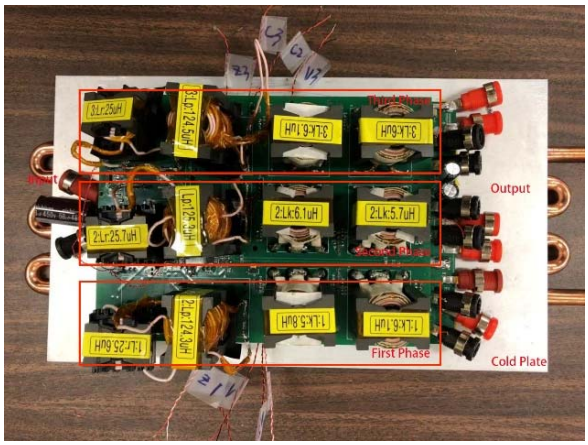

Fig. 10. Photo of the proposed LDC for EVs

Fig. 11 shows the experimental platform of the proposed LDC for EVs. DC supply Xantrex XDC600-20 is used to provide input power for the prototype, and three electronics loads in parallel are adopted to provide 270A load current.

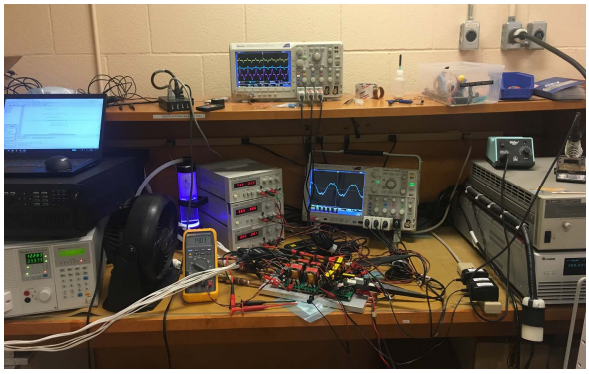

Fig. 11. Experimental platform

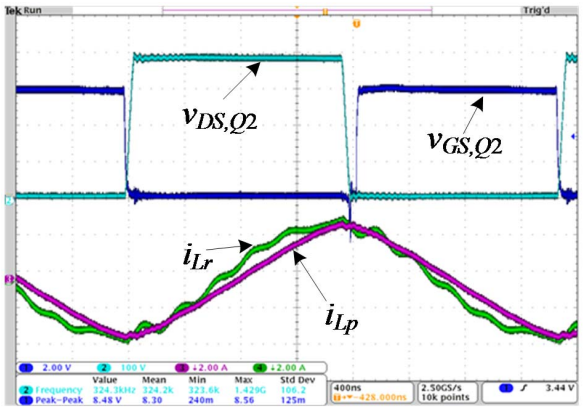

Fig. 12. ZVS turn-on of primary switches Q_2 at V_{in}=380V, V_{out}=14V and 10A load current

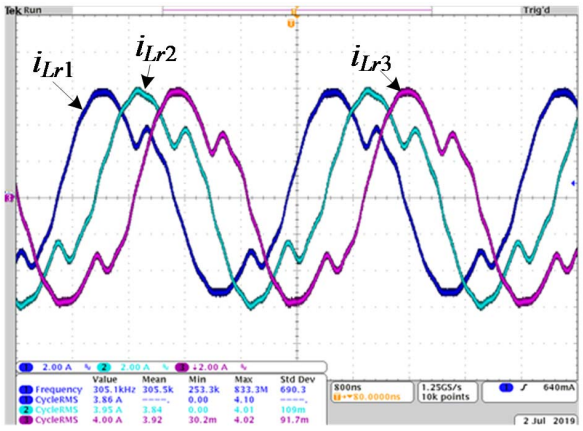

(a) resonant currents i_{Lr1}, i_{Lr2}, i_{Lr3}

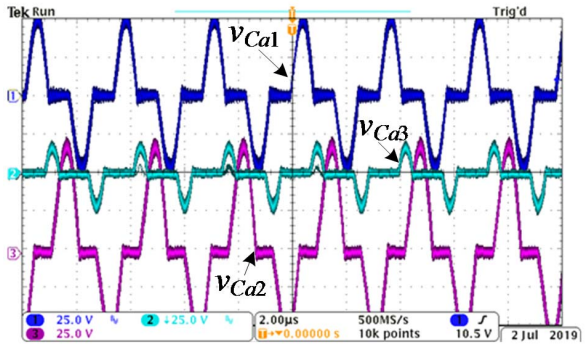

(b) voltages across capacitor C_{a1}, C_{a2} and C_{a3}

Fig. 13. Current sharing of the proposed LDC for EVs

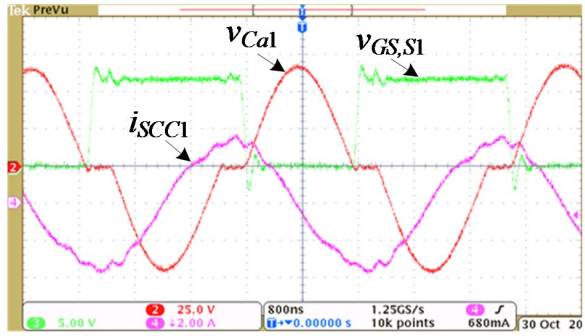

Fig. 14. SCC circuit waveforms of the proposed LDC

By properly designing the L_p value and adopting GaN HEMTs in primary, ZVS turn-on of primary switches can be achieved under light load. Fig. 12 shows ZVS turn-on of primary switches Q_2 at V_{in}=380V, V_{out}=14V and 10A load current.

As shown in Fig. 13(a), three phase circuits are interleaved with 60° phase difference. Although there is tolerance among the three phase magnetic components, the resonant currents of the LDC are balanced well by adjusting the conduction phase angle of the SCC when the input voltage is 380V and the output voltage is 14V at 270A load current. The switching frequency is 305kHz and peak current of resonant current i_{Lr1}, i_{Lr2}, i_{Lr3} are 6A, which is corresponding with the simulation results. As shown in Fig. 13(b), the voltage stress of the switches in three phase SCC are low with peak value of around 75V.

Fig. 14 shows SCC circuit waveforms of the proposed LDC. From waveforms of V_{Ca1}, $V_{gs,S1}$, i_{SCC1}, ZVS turn-on of switch S_1 is achieved, which verifies the analysis and simulation results.

Fig. 15 shows the efficiency of the proposed LDC. When the input voltage is 380V and output voltage is 14V, 95.8% efficiency is achieved at 270A load current, and peak efficiency is 96.5% at 160A load current.

Table II compares the LDC reported in literatures with the LDC developed in this work. In [1]-[5], the phase-shift full bridge DC-DC converter is adopted for LDC, it is difficult to achieve ZVS of switches at wide load range. [6]-[7] adopts single phase LLC DC-DC converter for LDC, high secondary current causes large loss when the converter operates at heavy load, thus low switching frequency can be used, and the power-density of the prototype is not high.

The proposed LDC adopts three phase LLC DC-DC converter, reduces current stress on switches, and high switching frequency is adopted, which achieves high efficiency and 3kW/L high power-density. 3.8kW high output power and wide input (250V~430V) and output (9V~16V) voltage range is realized, and only 1.5kg light weight is achieved in the proposed LDC, which improves the performance of LCD for EVs significantly.

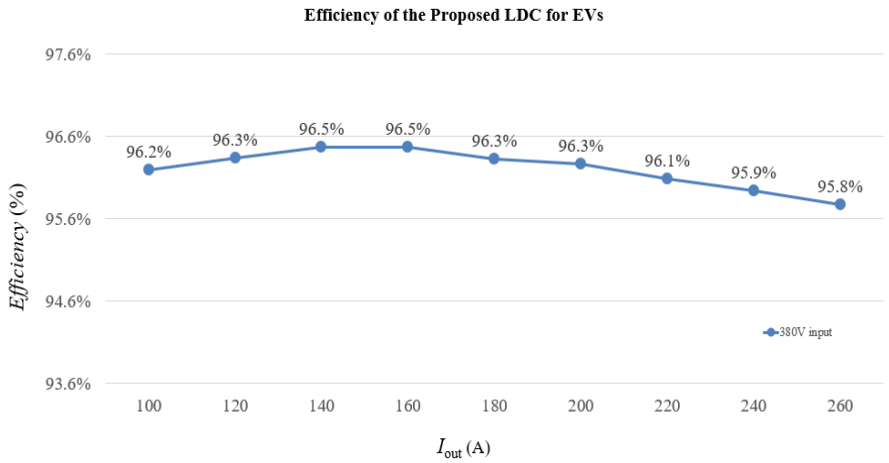

Fig. 15. Measured efficiency

TABLE II: COMPARASION BETWEEN THE PROPOSED LDC AND OTHERS LDC

Reference	Topology	Specification of the Converter						
		Input voltage	Output voltage	power	Peak efficiency	Full-load efficiency	Power density	Switching frequency
[1]	Phase-shift full bridge converter	200V~400V	12V	1.2kW	95.5%	90%	0.5kW/L	100kHz
[2]	Phase-shift full bridge converter	300V	12V	2kW	94%	93.2%	-	227kHz~297kHz
[3]	Phase-shift full bridge converter	235V~431V	11.5V~15V	2kW	93.5%	93%	0.94kW/L	200kHz
[4]	Phase-shift full bridge converter	300V~400V	12V~16V	0.72kW	93.5%	90%	-	100kHz
[5]	Phase-shift full bridge converter	250V~400V	13V~15V	1kW	93%	92%	-	100kHz
[6]	LLC converter	220V~450V	6.5V~16V	2.5kW	93.2%	92%	1.17kW/L	90kHz~200kHz
[7]	LLC converter	260V~430V	12.5V~14.5V	1.9kW	93%	91%	1.02kW/L	65kHz~150kHz
[8]	LLC converter	330V~410V	14V	2.5kW	95%	93%	1kW/L	250kHz
[9]	Two-stage converters	200V~400V	12V	2kW	95.9%	94.2%	-	100kHz~133kHz
The proposed LDC	SCC-LLC converter	250V~430V	9V~16V	**3.8kW**	**96.5%**	**95.8%**	**3kW/L**	260kHz~400kHz

VII. Conclusion

To reduce the conduction loss for low voltage high current application, a three-phase interleaved LLC DC-DC converter with SCC is designed for EV LDC in this paper. In the proposed LDC, GaN HEMTs are used in the transformer primary allowing for the switching frequency to be increased while the circuit volume is reduced. 250V~430V input and 9V~16V output wide voltage range, 14V 270A high load current is realized in the proposed LDC. ZVS turn-on of the primary switches and secondary SRs as well as the SCC switches is achieved. ZCS turn-off of secondary SRs is also realized. By adjusting the conduction phase angle of SCC, three phase resonant currents are balanced. The proposed LDC achieves an efficiency of 95.8% at 270A load current and a peak efficiency of 96.5% with a 3kW/L power-density and 1.5kg light weight, which has the best performance at the same specification products for EVs.

VIII. References

[1] Ruoyu Hou and Ali Emadi, "Applied integrated active filter auxiliary power module for electrified vehicles with single-phase onboard chargers," IEEE Transactions on Power Electronics, vol. 32, no. 3, pp. 1860-1871, Mar. 2017.

[2] Majid Pahlevaninezhad, Josef Drobnik, Praveen K. Jain and Alireza Bakhshai, "A load adaptive control approach for a zero-voltage-switching dc/dc converter used for electric vehicles," IEEE Transactions on Industrial Electronics, vol. 59, no. 2, pp. 920-933, Feb. 2012.

[3] Djilali Hamza, Majid Pahlevaninezhad, and Praveen K. Jain, "Implementation of a novel digital active EMI technique in a DSP-based dc–dc digital controller used in electric vehicle (EV)," IEEE Transactions on Power Electronics, vol. 28, no. 7, pp. 3126-3137, Jul. 2013.

[4] Ruoyu Hou and Ali Emadi, "A primary full-integrated active filter auxiliary power module in electrified vehicles with single-phase onboard chargers," IEEE Transactions on Power Electronics, vol. 32, no. 11, pp. 8393-8405, Nov. 2017.

[5] Yun-Sung Kim, Chang-Yeol Oh, Won-Yong Sung and Byoung Kuk Lee, "Topology and control scheme of OBC–LDC integrated power unit for electric vehicles," IEEE Transactions on Power Electronics, vol. 32, no. 3, pp. 1731-1743, Mar. 2017.

[6] Chen Duan, Hua Bai, Wei Guo and Zhong Nie, "Design of a 2.5-kW 400/12V high-efficiency dc/dc converter using a novel synchronous rectification control for electric vehicles," IEEE Transactions on Transportation Electrification, vol. 1, no. 1, pp. 106-114, Jun. 2015.

[7] Dong-Hee Kim, Min-Jung Kim and Byoung-Kuk Lee, "An integrated battery charger with high power density and efficiency for electric vehicles," IEEE Transactions on Power Electronics, vol. 32, no. 6, pp. 4553-4565, Jun. 2017.

[8] Gang Yang, Patrick Dubus and Daniel Sadarnac, "Double-phase high-efficiency, wide load range high- voltage/low-voltage LLC dc/dc converter for electric/hybrid vehicles," IEEE Transactions on Power Electronics, vol. 30, no. 4, pp. 1876-1886, Apr. 2015.

[9] Dongok Moon, Junsung Park and Sewan Choi, "New interleaved current-fed resonant converter with significantly reduced high current side output filter for EV and HEV applications," IEEE Transactions on Power Electronics, vol. 30, no. 8, pp. 4264-4271, Aug. 2015.

[10] Zhiyuan Hu, Yajie Qiu, Yan-Fei Liu and Paresh C. Sen, "A Control Strategy and Design Method for Interleaved LLC Converters Operating at Variable Switching Frequency," IEEE Transactions on Power Electronics, vol. 29, no. 8, pp. 4426-4437, Aug. 2014.